Original Paper

Indoor and Built Environment

Indoor Built Environ 2011;20;2:206–216

Accepted: September 19, 2010

Numerical Simulation and *In Situ* Investigation of Fine Particle Dispersion in an Actual Deep Street Canyon in Hong Kong

Yun-Wei Zhang[a] Zhao-Lin Gu[b] Shun-Cheng Lee[c]
Tzung-May Fu[c] Kin-Fai Ho[c]

[a]School of Energy and Power Engineering, Xi'an Jiaotong University, Xi'an 710049, China
[b]Department of Environmental Science and Technology, School of Human Settlements and Civil Engineering, Xi'an Jiaotong University, Xi'an 710049, China
[c]Department of Civil and Structural Engineering, Hong Kong Polytechnic University, Hung Hom, Kowloon, Hong Kong, China

Key Words
Aspect ratio · CFD simulation · Dispersion · Large eddy simulation · $PM_{2.5}$ · Reynolds number · Street canyon

Abstract
This paper reports a computational fluid dynamics simulation of airflow and fine particle ($PM_{2.5}$) dispersion in the street canyon in Hong Kong, using large eddy simulation. An aspect ratio (AR) of 2.7 and a Reynolds number of 5×10^6 with a one main vortex, were used. This study focused mainly on the vehicle-induced momentum source and $PM_{2.5}$ concentrations were measured at 10 altitudes near the leeward wall in the street canyon, to provide high resolution measurements for model validation. The simulated $PM_{2.5}$ concentrations agreed well with the measurements, ($R = 0.85$). The concentration was higher at the lower part near the leeward wall than the upper part. Higher concentration was found near the roof level. A near-uniform vertical dispersion of $PM_{2.5}$ near the windward wall was demonstrated; and the average concentrations were lower than found near the leeward wall. The intermittent escape of the $PM_{2.5}$ above the canyon at the roof level occurred mainly at the centre and near windward wall areas. The results demonstrated that a reduction in the AR can be conducive to pollutant dispersion in street canyon planning. The findings of this research would inform building designers to formulate effective strategies such as positioning of ventilation air intake, for the control of ingress of $PM_{2.5}$ into building environments.

Introduction

The link between certain respiratory health issues, such as the increase in asthma cases and mortality, and

Los Angeles, London, New Delhi, Singapore and Washington DC
DOI: 10.1177/1420326X10387694
Accessible online at http://ibe.sagepub.com

Prof Zhao-Lin Gu,
Department of Environmental Science and Technology, School of Human Settlements and Civil Engineering, Xi'an Jiaotong University, 28 Xianning West Road, Xi'an 710049, China, Tel. +86 29 8339 5100, Fax. +86 29 82665111,
E-Mail guzhaoln@mail.xjtu.edu.cn

suspended particulate matter (PM) in the atmosphere, especially in urban environments have been established by epidemiological and toxicological studies [1–3]. The dominant sources of $PM_{2.5}$ are from the traffic emissions [4,5]. The concentrations of PM in the outdoor environment and ventilation intake would have a serious effect on the indoor concentrations and exposure of building occupants [6–12]. The indoor exposure risk based on realistic scenarios has also been reported [13–15].

Concentrations of high pollutants inside street canyons could also have an impact on indoor air quality [16–22]. It is therefore important to understand the dispersion characteristics of pollutants in the street canyons under various urban meteorological conditions, to formulate effective strategies such as positioning of ventilation air intake, for emission control; and for urban planning. Several methods, such as laboratory scale experiments [17,19], *in situ* measurements [23,24], computational fluid dynamics (CFD) simulations [20–22], have been used to investigate airflow and $PM_{2.5}$ dispersion in street canyon.

Street canyon modelling methods have been reviewed by Vardoulakis et al. [18]. The CFD method has been widely used to simulate airflow in street canyon [20–22,25–28]. In particular, large eddy simulation (LES) is a technique used to evaluate the unsteadiness and intermittency characteristics of turbulent flow within street canyon. The aspect ratio (AR) of building height (H) to street width (W) is used to describe the characteristics of the geometric condition of a street canyon. In this paper, the street canyon with an AR exceeding 2 would be described as the deep street canyon. The Reynolds number (Re) is a dimensionless number used to describe the turbulence within a street canyon. Re is calculated using the reference wind velocity and the height of buildings on either side of the street canyon.

In recent years, with the increase in computer capability, the LES methods have been widely used to study the turbulence and pollutant distribution and dispersion within the urban street canyons [25–27]. Most CFD models, currently being used to study the flow and turbulence within street canyons, are mainly employed in the laboratory scale simulation using wind tunnel and buildings are scaled to several centimetres, with a Re of around 10^4. However, in actual street environment, the Re would be around 10^6–10^7 [28,29]. In fact, two or more main vortices could be observed in the laboratory scale models of deep street canyons [30]. However, in actual site monitoring reported by Eliasson et al. [29] showed only one main vortex was observed in such deep street canyons. As multiple vortices can restrict pollutant dispersions, laboratory scale model would fail to simulate the actual wind flow and pollutant distribution inside real deep street canyons. Yang and Shao [28] simulated the flow and pollutant distribution in actual street canyons using a Re of 6×10^5. The effect of street canyon AR on flow was determined and only one main vortex for canyons with AR up to 2.5 was observed. However, the wind turbulence and pollutant dispersion characteristics were not investigated by this study.

To characterise the flow structures in street canyon simulations, the critical Re is used. Several critical Re's have been reported, such as 3400 [31]. However, these Re's were obtained from wind tunnel experiments, where the street canyons AR were around 1. As pointed out by Uehara et al. [32], the critical Re should rely on the sizes and shapes of the street canyon models. The commonly known critical Re's are not suitable in deep street canyon simulations, thus the real scale simulation should be used.

In real scale models, effects of vehicle flows on wind momentum and turbulence should be considered [33]. Solazzo et al. [34] studied the effects of vehicle flows by adding a vehicle-induced turbulence model in their wind tunnel experiment and CFD model. Their results found that, with vehicle-induced turbulence model, the maximum wind velocities near the ground and windward wall were larger than without vehicle-induced turbulence model. The increase of velocity near ground and windward wall would conduct the wind flow from the upper part down into the street canyons, and would therefore change the wind flow and turbulence distribution. In this study, a vehicle-induced momentum source model was used to evaluate the dispersion of $PM_{2.5}$ within the street canyon.

A well-developed LES model should have an accurate subgrid-scale stress (SGS) model, which would provide simulations of the effect on turbulence dissipation. Most currently used SGS model use a grid width to approximate the characteristic length of SGS motions to calculate the vortex viscosity coefficient [35]. The characteristic length of SGS motions should be flow dependent [26]. However, the grid width is a geometrical length scale and this would depend on the actual implementation of LES. Qiu et al. [36] improved on Sagaut's mixed scale model by computing the SGS characteristic length self-adaptively, and obtained satisfactory spatial distribution of the SGS motions. For the airflow within a street canyon, the SGS characteristic length inside the canyon is different to that above the canyon. Cui et al. [26] used different Smagorinsky constants to coordinate with the change of

SGS characteristic lengths. In this study, the SGS characteristic length was calculated, self-adaptively.

Particle transfer model is also important for $PM_{2.5}$ dispersion simulations. One of the Eulerian methods, the drift flux (DF) model has been successfully used for modelling particle distribution and deposition in indoor environments [37,38], but rarely used in $PM_{2.5}$ dispersion simulation in street canyons. DF models assume the gaseous and particulate phases are well mixed and a small drift velocity consisting of gravitational settling and diffusion would be allowed between the particles and bulk air. Most currently used CFD models do not consider the gravitational settling [27,28]. The DF model is incorporated in this study to represent, more accurately, $PM_{2.5}$ dispersion in street canyons.

Measurement studies of pollutant dispersion in street canyons are mostly carried out in laboratory wind tunnels [39,40]. Measurements of PM dispersion in actual street canyons are much less common [23,29,41,42]. All of these measurement studies failed to achieve a sufficiently high spatial resolution of PM distribution measurements necessary for validating numerical models [42]. Chan and Kwok [23] measured PM_{10} concentration at four altitudes spaced 28.5 m apart, while Colls and Miccallef [41] measured PM_{10} concentration only in the lower part of the street canyon. Comparative study carried out by Kumar et al. [42] measured the particle number concentration at four altitude levels on the leeward wall of an uniform street canyon; the measurements were then compared with the simulated results by empirical models (OSPM and box model) and a 2D CFD model. In order to consider the effects of wind shear at roof level and the complicated turbulence near ground, measurement study with higher spatial resolution should be carried out.

Field Measurement

Site Description

Measurements were carried out in an old residential district, on Yu Chau Street, Sham Shui Po, Kowloon, Hong Kong (22°19′N and 114°09′E). Yu Chau street, extending from the southeast (SE) to northwest (NW) with a one-way traffic (SE to NW), represents a typical deep street canyon in Kowloon, Hong Kong. The section of the street canyon studied was about 100 m long (L), with an AR of approximately 2.7 ($H = 27$ m, $W = 10$ m). Measurements were taken 30 m away from the intersection at the SE end of the section. The nearest tall building (about 36 m in height), was located about 45 m away from the measurement point at the NW end. The aerial photograph of the measurement site is as shown in Figure 1(a). Buildings along the street were symmetrical in height, with flat roofs, thus allowing simple representation of the computational domain for simulation (Figure 1(b)).

Instrumentation and Measurements

Two DustTrak air monitors (Model 8520, TSI Inc., US) were used to monitor $PM_{2.5}$ concentration at different height levels pseudo-simultaneously. The term "pseudo-simultaneously", means that each cycle of sampling were carried out when the traffic flow and meteorological condition were comparatively steady [42]. During each cycle, the two DustTraks were moved from level to level to measure $PM_{2.5}$ concentrations at the respective locations. DustTrak monitor can provide a direct reading of laser light scattering by the particle aerosols. DustTraks were calibrated against a filter-based sampler, BGI prior to the monitoring to ensure accuracy of measurements.

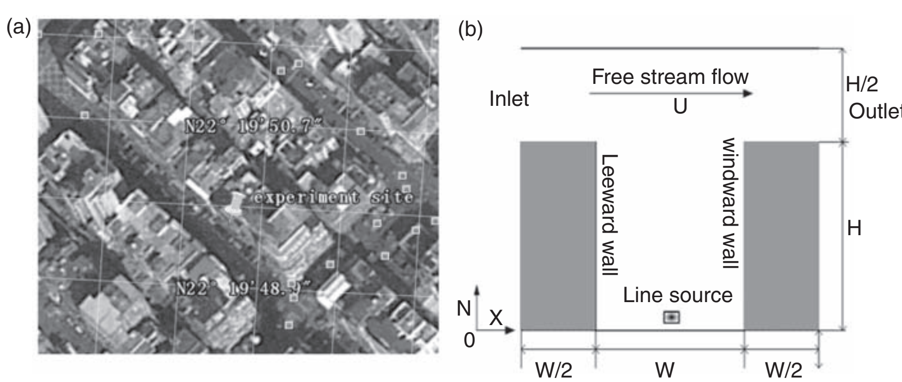

Fig. 1. (a) Aerial photograph of the measurement site; (b) schematic diagram of computational domain that represents Yu Chow Street (crossstreet section).
Note: The pointer in centre of Figure 1(a) shows the measurement site.

The Dust Traks had been found to overestimate the $PM_{2.5}$ concentration by 1.2 times by this study. Overestimations of $PM_{2.5}$ concentration by Dust Trak in street canyon measurements have also been reported by Wu et al. [43] in Macao.

Samples were collected from 17:00 to 19:00 between 27 April and 1 June, 2009. Meteorological parameters: wind speed and wind direction were measured at 2 m above the building roof using a sonic anemometer (Wind Sonic, Gill Instruments). Traffic composition and volume were determined by manual counts at the sampling site at 15-min intervals during the sampling periods. The vehicle types were classified as:

- diesel vehicles (DV) – buses, heavy-goods trucks and light-goods trucks; and
- non-diesel vehicles (NDV) – motorcycles, private cars, LPG-fuelled taxis and minibuses.

Measurements were made pseudo-simultaneously at 10 different height levels, from ground to roof, in one sampling cycle. The 10 sampling points were located along a vertical straight line about 0.4 m away from the walls of the buildings within the street canyon at heights of 1.2, 3.7, 6.7, 9.7, 12.7, 15.7, 18.7, 21.7, 24.7 and 27.1 m, respectively. The sampling point at 27.1 m was above the canyon top level. The DustTraks were used to measure $PM_{2.5}$ at a different sampling level in every 5–10 min.

This study was about the airflow and pollutant distribution in a deep street canyon, when wind circulation was dominating the street canyon airflow. A relatively steady meteorological condition, a high wind speed with a near perpendicular flow to the street was required for this monitoring study [42]. The measurement results of 11 May, 2009 were selected for comparison with the modelled results. These measurements were made in a period when the main wind direction was blowing from the northeast across the canyon at an average wind speed (reference velocity) of $2.05\,m{\cdot}s^{-1}$. The Re used was based on this reference velocity and the building height (H) was 5×10^6. At this speed, the wind was strong enough to drive one or more vortex circulations inside the street canyon, as shown by Eliasson et al. [29]. Vehicle flows were 148 and 155 during the measurement time at 17:10 to 17:25 and 18:00 to 18:15, respectively. The percentages of DV were 33.1% and 34.8%, respectively during those times. According to observations, during the time period, 17:00 to 19:00, the ambient wind and traffic flow remained consistently steady. All sampling points were on the leeward side of the canyon and no measurements were made on the windward side.

Measurement Results

Figure 2 shows the measured vertical profile of $PM_{2.5}$ at the leeward wall. DustTracks exported one average concentration data per minute for data recording. At each height level, 5 to 10 $PM_{2.5}$ concentrations were collected. Figure 2 shows the average $PM_{2.5}$ concentrations and their deviations. $PM_{2.5}$ concentrations decrease with height, and this was consistent with the findings from Chan and Kwok [23]. In this study, $PM_{2.5}$ concentration was shown to decrease at the 3.7 m height level by 31.95%, compared to that at the 21.7 m level.

Discussion

This measured $PM_{2.5}$ vertical profile shown in Figure 2 was consistent with that of Kumar et al.'s [42] findings. Kumar et al. measured the maximum value of ultrafine particle concentration at a height of 2.2 m, similar to our measurement.

A local maximum in $PM_{2.5}$ concentration was observed near the top of the street canyon (at the height of 24.7 m), which has so far not been reported in literature. The reason was probably due to the measurements were made under low vertical resolution, and therefore would not illustrate the vertical distribution in $PM_{2.5}$ concentration in detail. The local maximum was due to the strong shear layer at the roof level above the street canyon. Because of the strong shear layer would drive a second order vortex at the up corner of the leeward wall [26], and this could confine the dispersion of

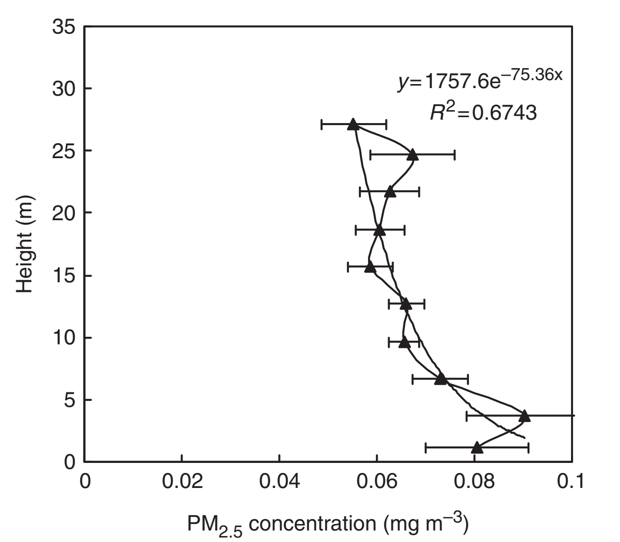

Fig. 2. Measured vertical profile of $PM_{2.5}$ concentrations (C) at the leeward wall.
Note: ▲ indicates the average concentration and horizontal bar indicates the deviation.

the pollutant. The following simulations demonstrate the second-order vortex phenomenon.

Numerical Model Formation and simulations

LES Model for Airflow Simulation

Governing Equations for the Resolved Field:

LES was used to simulate flow and turbulence distributions, assuming incompressibility. By applying the top-hat (box) filter to Navier–Stokes equations, the governing equations for LES were obtained in the form of continuity equation (Equation (1)):

$$\frac{\partial \overline{u_i}}{\partial x_i} = 0 \tag{1}$$

and the momentum equations (Equation (2)):

$$\frac{\partial \overline{u_i}}{\partial t} + \frac{\partial\left(\overline{u_i}\,\overline{u_j}\right)}{\partial x_j} = -\frac{\partial \overline{p}}{\partial x_i} - \frac{\partial \tau_{ij}}{\partial x_j} + \frac{1}{\mathrm{Re}}\frac{\partial^2 \overline{u_i}}{\partial x_j \partial x_j} + S_i \tag{2}$$

where, $\overline{u_i}$ and $\overline{u_j}$, are the resolved-scale velocities in i and j directions, $\overline{p}$ the resolved-scale virtual pressure, τ_{ij} the SGS and S_i the additional source term, which contains all the other terms not explicitly appeared in these equations [44].

Equations (1) and (2) were expressed in tensor notation so that the indices i and j would range over the spatial dimensions. The reference length scale W (street width) and the reference velocity U (the average measured velocity at 2 m above the roof level) were used to derive Equations (1) and (2) in dimensionless terms.

Subgrid-Scale Stress Model:

In this study, the modified and improved Smagorinsky SGS scheme [45] by using Qiu et al.'s [36] method to compute the characteristic length dynamically was used. In Smagorinsky SGS scheme, the SGS terms in the governing equations can be parameterised as shown in Equations (3) and (4):

$$\tau_{ij} = -2\nu_{\mathrm{sgs}}\overline{S}_{ij} + \frac{1}{3}\tau_{kk}\delta_{ij} \tag{3}$$

$$\nu_{\mathrm{sgs}} = \left(C_{\mathrm{s}}\right)^2\left(C_L\overline{\Delta}\right)^2\left|\overline{S}\right| \tag{4}$$

where, C_{s} is the Smagorinsky model constant, ν_{sgs} the SGS viscosity and C_L the modification coefficient for the SGS characteristic length. The detailed computational process was reported by Qiu et al. [36].

Particle Transfer Source Emission Model:

The DF model was used here to simulate particle transfer in street canyon area and account for the finite particle inertia. The DF model is described by Equations (5) and (6), as follows:

$$\frac{\partial \overline{c}}{\partial t} + \frac{\partial\left(\left(\overline{u_i} + \delta_{i,3}Vs\right)\overline{c}\right)}{\partial x_i} = \frac{\left(\nu + \nu_{\mathrm{sgs}}\right)}{Sc}\frac{\partial^2 \overline{c}}{\partial x_i \partial x_i} + S_0 \tag{5}$$

$$V_{\mathrm{S}} = \frac{\rho_P d^2 g C_{\mathrm{c}}}{18\eta} \tag{6}$$

where $\overline{c}$ is the resolved-scale $PM_{2.5}$ concentration, S_0 the $PM_{2.5}$ emission source, Sc the Schmidt number, $\delta_{i,3}$ the Kronecker delta, V_{s} the average settling velocity calculated by Equation (6) and C_{c} the slip correction factor [46].

The particle diameter d was set to be 1.0 μm, which is the mode of particle size distribution of $PM_{2.5}$ found in Hong Kong based on previous measurements [28]. Considering the gravitational sedimentation effect, this particle transfer model has the capacity to simulate the dispersion of multi-diameter distribution particle system.

The $PM_{2.5}$ emission factor (EF) was calculated using tunnel experimental data reported by Cheng et al. [47]. This EF was defined as the mass of specific pollutants produced in a unit kilometre, and calculated in unit of $\mathrm{mg{\cdot}m^{-1}{\cdot}vehicle^{-1}}$ by Equation (7), as:

$$\mathrm{EF} = 0.0699 \times \mathrm{NDV\%} + 0.1250 \times \mathrm{DV\%} + 0.0449 \tag{7}$$

where, NDV% and DV% represent the percentages of NDV and DV, respectively.

Vehicle-Induced Momentum Source Model:

The Eulerian–Lagrangian model for traffic dynamics as described by Katolicky and Jicha [48] was used in our CFD modelling of the traffic-induced momentum source. In the simulation by the Eulerian–Lagrangian model, moving cars were treated as discrete objects that "fly" through the computational domain. These discrete objects would be treated with a Lagrangian momentum equation (Equation (8)) and their velocities would be solved along their trajectories.

$$\frac{\mathrm{d}\vec{U}_V}{\mathrm{d}t} = \frac{1}{\tau_{\mathrm{M}}}\left(\vec{U}_\infty - \vec{U}_{\mathrm{V}}\right) \tag{8}$$

where, $\vec{U}_{\mathrm{V}}$ is the vehicle velocity, $\vec{U}_\infty$ the ambient wind velocity and τ_{M} a so-called relaxation time for vehicle [48].

The change in the velocity of the vehicle should be regarded as a virtual change in the modelling.

By integrating Equation (8) under the assumption that the relaxation time would be constant over a time step and this would yield Equation (9) as in the following:

$$\vec{U}_{V1} = \vec{U}_{V0} \exp\left(\frac{-\Delta t}{\tau_M}\right) + \vec{U}_{\infty}\left(1 - \exp\left(\frac{-\Delta t}{\tau_M}\right)\right) \quad (9)$$

where, $\vec{U}_{V0}$ and $\vec{U}_{V1}$ are the vehicle velocities at the beginning and the end of the time step$t$, respectively. The momentum change ($\vec{H}_V$) of the vehicles can be calculated according to Equation (10):

$$\Delta\vec{H}_V = m_V\left(\vec{U}_{V1} - \vec{U}_{V0}\right) \quad (10)$$

where, m_V is the mass of the vehicle.

When calculating the additional source term S_i in Equation (2) to account for the interaction between vehicles and the ambient air; the vehicle-induced momentum changes in air as $-\vec{H}_V$ was calculated and also provided the average of all the momentum changes in the grids when the vehicles passed by. As vehicles were moving at a constant speed; the changes in the vehicle velocity as shown in Equations (8), (9) and (10) would be regarded as virtual changes. This would mean that the vehicle velocity should be reset to be the original value at the end of every time step.

Computational Domain, Boundary Condition and Solution:

The height and width of the computational domain were set to be $1.5H$ and $2W$, respectively, as illustrated in Figure 1(b). A non-uniform grid system [49] was used, with a minimum grid width value of $0.00828W$ in the across-street direction near the building walls. The canyon was modelled as an infinitely long canyon with a cross-wind condition, and the spanwise (along street) length (L) was set to be $2H$ with periodic boundary condition. A line source located at the centre of the canyon was used to represent the vehicle emission (Figure 1(b)). The initial value of the wind velocity was set to be zero inside the canyon. The reference wind speed at 2 m above the roof level was set to $U = 2.05\,\mathrm{m{\cdot}s^{-1}}$, with wind speed increasing exponentially with height above the building roof. Initial $PM_{2.5}$ concentration was set to be zero, and the source emission was switched on at the 2500 time step (approximately 8.3 min into the simulation) after the flow reached a steady state.

Periodic boundary conditions for velocities were in the across-street and spanwise directions, while free boundary condition was used at the top boundary position. Non-slip wall condition was used for the determination of wind velocities at all solid walls. The concentration of $PM_{2.5}$ was set to be zero at the inlet, and the open boundary condition was set at the outlet (Figure 1(b)). However, for the high Re flow in this study, there was little prospect of resolving the viscous sublayer on the solid walls. Thus, a wall function, as illustrated by Walton and Cheng [49] was used.

The resolved-scale dynamic equations of the mathematical model were solved by the finite volume method (FVM), with the SIMPLE algorithm [44] used to deal with the implicit dependence of velocity and pressure. A bounded central discretisation (BCD) method was used to determine the advection terms of the momentum equations, with the first-order upwind scheme used when the convective boundedness criterion (CBC) was not satisfied [44].

Scale Effect on Flow Pattern in Deep Street Canyons

Laboratory scale CFD modelling (with Re around 10^4) [50] and laboratory scale water channel tests [30] have shown multiple vortices that could exist inside deep street canyons with an $AR = 2$. However, actual site observations by Eliasson et al. [29] and actual scale simulation by Yang and Shao [28] ($Re = 6 \times 10^5$) showed that there were only one main vortex in deep street canyons with an AR up to 2.5. In this study, the commonly known critical Re was assumed to be 3400 based on street canyons with AR around 1 and therefore would not be suitable for deep street canyon simulations. The scale effects on airflow patterns in deep street canyon simulations should be studied.

In order to show the scale effects on airflow patterns in deep street canyons, the airflow in a street canyon with AR 2 was simulated in both laboratory scale ($Re = 15{,}000$; with $U = 2\,\mathrm{m{\cdot}s^{-1}}$, $H = 9\,\mathrm{cm}$) and real scale ($Re = 5 \times 10^6$; with $U = 2\,\mathrm{m{\cdot}s^{-1}}$, $H = 30\,\mathrm{m}$). In laboratory scale models (wind tunnel simulation), the reference velocity is usually set to be several metres per second, which is similar to that measured in field experiments. However, building dimensions are set on tens of centimetres, which is far smaller than the real building scales. Thus, a fixed reference wind velocity and different building heights were used in this study, which would be consistent with the real situation.

The vertical distribution of horizontal velocity at the centre of the street canyon that simulated in both laboratory scale and real scale in this work are shown in Figure 3. The findings of our CFD laboratory scaled

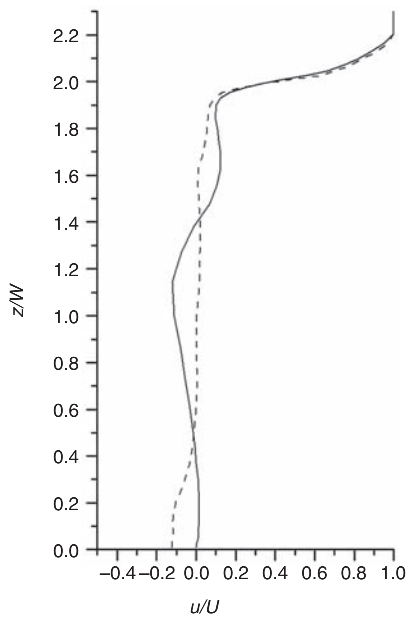

Fig. 3. Comparison of the vertical profiles of horizontal velocities found at the centre of the street canyon simulated in different Re's. Notes: The dashed line represents data from our real scale CFD simulation ($Re = 5 \times 10^6$); while the solid line represents data from our laboratory scale CFD simulation (Re = 15,000).

modelling simulations also showed two counter flow vortices and this agrees well with the results reported by Li et al. [50,30], illustrating the appropriateness of the CFD modelling method for assessing airflow in street canyon.

In the simulation results, only one main vortex was shown inside the street canyon under real street canyon conditions (Figure 3). This real scale simulated flow pattern inside the deep street canyon (with an AR 2) agrees well with work reported by Eliasson et al. [29] and Yang and Shao [28], and this confirmed our assumption that the commonly known critical Re was not suitable for deep street canyon simulation.

The issue of laboratory versus real scale simulation is important because the airflow pattern inside deep street canyons can affect the pollutant distribution significantly. Flow vortices would cause pollutant to circulate inside street canyons and confine pollutants in the lowest circulation. So, the multi-vortex flow structure would cause large vertical gradient of pollutant concentrations inside the deep street canyons [50]. As laboratory scale and real scale simulations can give very different results; the simulation of airflow and pollutant dispersion in actual deep street canyons, real scale models should be used, which means the Re should be set to around 10^6–10^7.

Simulated Flow and Turbulence Distributions in Yu Chau Street Canyon

Figure 4(a) and (b) show the velocity and turbulence distribution simulated by the CFD modelling of dispersion in Yu Chau street canyon. The mean velocity vectors and stream lines illustrated clearly a single primary vortex that could occur inside the street canyon. Figure 4(a) shows a secondary vortex occurred near the top of the leeward wall; this was caused by the strong sheer layer on the top level of the street canyon. Figure 4(b) shows the distribution of turbulent kinetic energy (TKE). Peak TKE values occurred at the windward side of the roof level. This characteristic TKE distribution is consistent with the simulations produced by Walton and Cheng [49] in a street canyon with an AR 1.2.

Comparison of the Measured and Simulated $PM_{2.5}$ Vertical Profiles

For the simulation of the vertical distribution of $PM_{2.5}$ along the leeward wall, the data were averaged during 80 dimensionless times. Both the simulated and measured results were normalised by Equation (11), in order to coordinate with the normalised velocities.

$$C^* = \frac{(C - C_b) \cdot U \cdot W}{EF \cdot N_V/3600} \tag{11}$$

where C^* is the normalised $PM_{2.5}$ concentration, C the averaged $PM_{2.5}$ concentration, C_b the background $PM_{2.5}$ concentration, EF the emission factor, N_V the vehicle flux in vehicle/h and U and W the reference velocity and street width, respectively.

The background $PM_{2.5}$ concentration was measured 2 m above the upwind side of the building roof, while it was set to be zero in simulation. Figure 5 shows the normalised $PM_{2.5}$ concentrations from measurement and simulation, plotted against the normalised height (z/W) in the canyon. Both the measured and simulation results show that normalised $PM_{2.5}$ concentrations were high near the bottom of the leeward wall (around 30), declined sharply with the rising height, and increased again in the upper area of the street canyon. The local rise of $PM_{2.5}$ concentration in the upper area near the leeward wall was likely due to the shear layer occurring at the roof level. Pollutants were confined by the second-order vortex occurring at the upper corner of the leeward wall (Figure 4(a)). These results show the ability of our newly

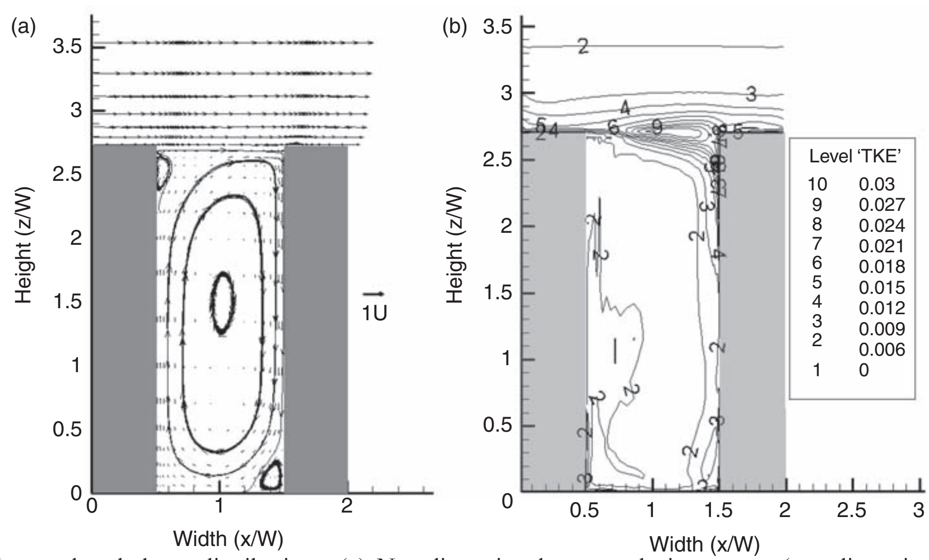

Fig. 4. Simulated flow and turbulence distributions. (a) Non-dimensional mean velocity vectors (non-dimensionalised using reference velocity U) and stream lines. (b) distribution of non-dimensional turbulence kinetic energy (non-dimensionalised using U^2, levels are labelled by level number instead of the TKE value).

developed CFD model consisting of the particle transfer and source emission model for simulation of dispersion of $PM_{2.5}$ concentration in detail.

A good correlation between the measured and modelled $PM_{2.5}$ concentrations ($R = 0.85$) was found, and this is shown in Figure 6. Regression analyses show that the model underestimated $PM_{2.5}$ concentration by 28.2% (Figure 6), which was probably caused by the underestimation of the EF. Li et al. [50] simulated the scalar (air pollutant) distribution in a deep street canyon in a laboratory scale model and produced a similar AR (3) to this study being reported here (2.7). Li et al. found three vortices inside the street canyon in their simulation work, and the normalised scalar concentrations varied from more than 2000 (at the lower end) to 20 (at the roof) near the leeward wall. The normalised scalar concentrations simulated by Li et al. [50] were clearly too large at the lower end of the leeward wall, compared with our measurement and real scale simulation. So, for flow and pollutant dispersion simulation in actual deep street canyons, real scale models would be more accurate than laboratory scale models.

The maximum $PM_{2.5}$ concentration measured near the leeward wall occurred at the 3.7 m height level; while in the simulation, the maximum concentration was found close to the road level near the leeward wall. At the road level in a real street canyon, the airflow would be more turbulent due to the turbulence induced by the traffic and temperatures of vehicles exhausts and the road surface. Vehicle exhausts would be diluted quickly by the airflow and then be transported to the leeward wall. Hence, the measured $PM_{2.5}$ concentration near the leeward wall surface was more "well-mixed" than that found by the model. Although the vehicle-induced momentum source on the flow pattern was accounted for in the model simulation, inside the street canyon, the turbulence effect was still underestimated as shown by the results.

Pollutant Distribution and Dispersion

As was shown in Figure 5, $PM_{2.5}$ concentrations near the windward wall were lower than at the concentration near the leeward wall and no obvious variation in concentration was associated with wall height. Our findings were consistent with the findings reported by Cai et al. [25] and Kumar et al. [42], which reported only one main vortex existed inside the street canyons studied. $PM_{2.5}$ concentrations at the windward wall were lower than near the leeward wall and this was due to the transportation effect of the single vortex structure. Another reason would be the removal of $PM_{2.5}$ pollutants at the roof level. Thus, pollutant circulation would be weaker near the windward wall.

As shown in Figure 4(b), the exchange of pollutants was mainly caused by the turbulent processes due to the

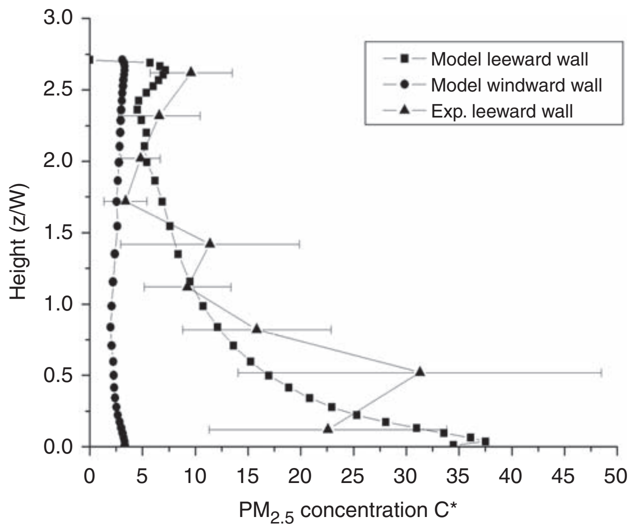

Fig. 5. Comparison of the measured data with the simulated vertical distribution profiles of the normalised $PM_{2.5}$ concentrations.

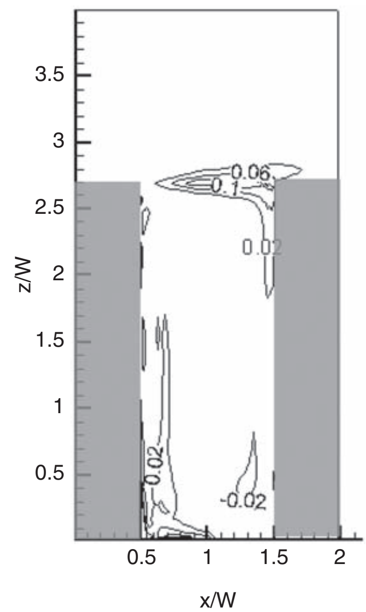

Fig. 7. Spatial distribution of the turbulent flux of $PM_{2.5}$ $\langle w'C^{*\prime}\rangle$.

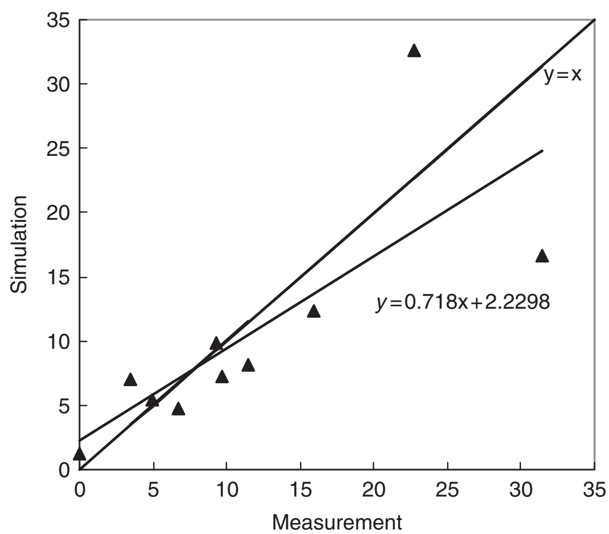

Fig. 6. Relationship between simulated and measured, normalised $PM_{2.5}$ concentrations found near the leeward wall.

horizontal mean flow at the roof level. This finding was consistent with that reported by Walton and Cheng [49] in a street canyon with AR 1.2.

The temporally averaged vertical pollution turbulence transport flux $\langle w'C^{*\prime}\rangle$ is shown in Figure 7. The figure shows large positive values at the roof level, with the maximum value closer to the windward side. The maximum pollution turbulence transport flux value was around 0.1. This was lower than the simulation found by Walton and Cheng [49], where the maximum value was about 1. This difference of maximum pollution turbulence transport flux value was probably due to the AR of the simulated street canyon. The comparison of values has illustrated that the simulation of pollutant dispersion in deep street canyons would be more difficult than that in shallow street canyons. Thus, in street canyon planning, reduce the AR would be conducive to pollutant dispersion.

The dispersion processes of $PM_{2.5}$ were illustrated by studying the typical temporal evolution of the normalised $PM_{2.5}$ concentrations as shown in Figure 8. $PM_{2.5}$ pollutants would accumulate in the lower corner of the leeward wall at dimensionless time ($T = WU^{-1}t^{-1}$) $280T$, and then travel up along the leeward wall in puffs intermittently, at time $282T$ and $286T$. When puffs of pollutants reach the top of the leeward wall, these tend to accumulate and then advected to the windward wall by the shear layer occurring at the roof level. Walton and Cheng [49] showed that the pollutants could acquire sufficient momentum at the roof level, and then push through the shear layer and into the free air aloft. That is, the large scale turbulence eddies would remove pollutants from the canyon rather than a steady diffusion resulting from small scale turbulence. In our simulation, the escaping of pollutants mainly happened at the roof level in the middle and near the windward wall of the street canyon, where the TKE value was large (Figure 4(b)). Our result agrees well with Walton and Cheng's [49] finding.

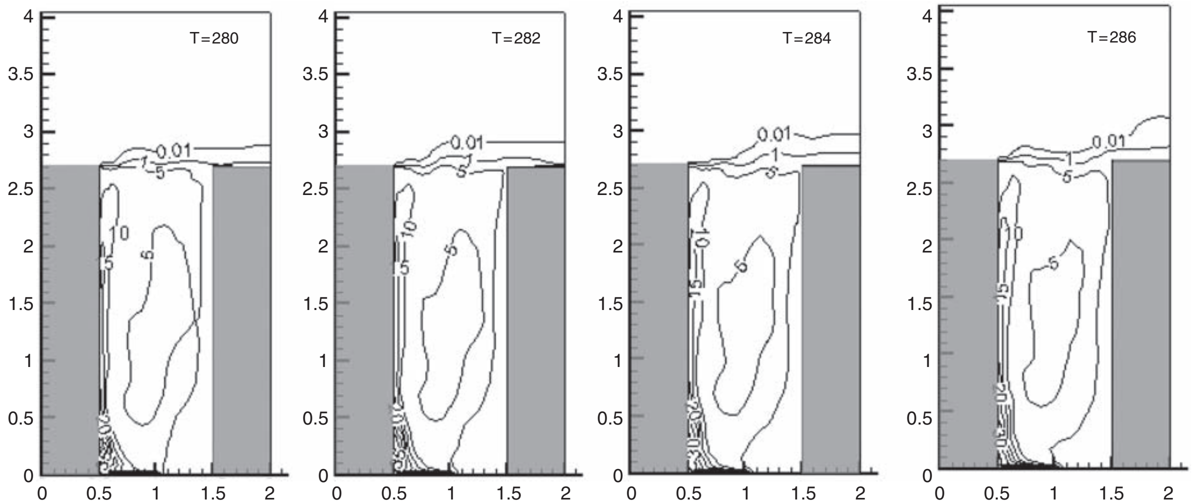

Fig. 8. Typical temporal evolution of the normalised $PM_{2.5}$ concentrations.
Note: T is the dimensionless time ($T = WU^{-1}t^{-1}$).

Conclusion

In this paper, a new CFD modelling method has been developed using LES. This CFD model can be used to simulate the flow inside deep street canyons in the point of view of laboratory scale and real scales, with an AR 2. The model would provide a mechanism to investigate scale effects on flow pattern in deep street canyons. The results of the laboratory scale simulation showed good agreement with previous simulations and measurements by other workers. Two primary vortices were found by this study.

The real scale simulation found only one primary vortex. The critical Reynolds numbers based on street canyon with AR 1 would not be suitable for deep street canyon simulation. So, for flow and pollutant dispersion simulation in actual deep street canyons, real scale models would be more accurate than laboratory scale models.

Using the newly developed CFD model in the simulation of Yu Chau street canyon in Hong Kong, with an AR of 2.7 and a Reynolds number around 5×10^6; the air masses would flow from the upper atmospheric level and circulate down to the bottom of the street canyon. The flow pattern illustrated a single primary vortex existed inside the street canyon and this was confirmed by comparison with the results of previous studies.

The CFD model also has the ability to capture the TKE distribution and turbulence intermission, with the maximum values occurring at the roof level of the street canyon.

The simulation of $PM_{2.5}$ distribution and dispersion in Yu Chau Street was consistent with the on site measurements. The computed vertical profile of $PM_{2.5}$ near the leeward wall correlated well with the measurement results with a correlation, $R = 0.85$.

Comparison of our simulation and measurement results with previous studies showed that, real scale models can be more accurate than laboratory scale models, for flow and pollutant dispersion simulation in actual deep street canyons.

Both the numerical and experimental data illustrated the vertical variation of $PM_{2.5}$ concentrations near the leeward wall in detail. The unexpected local maximum near the top of the canyon could be related to the shear layer at the roof level and the second order vortex occurring at the upper corner of the leeward wall.

The temporal simulations of the pollutant concentration indicated that puffs of pollutants would move away from the canyon to the free air aloft in an intermittent way.

Further improvement of the present model would focus on the turbulence simulation near the road level. An accurate vehicle-induced turbulence model and considerations of temperature effects should also be included.

Acknowledgements

This study was financially supported by the National Natural Science Foundation of China (no. 10872159), Interdisciplinary Programmes of Xi'an Jiaotong University (2009xjtujc10) and Joint Education Project of Hong Kong Polytechnic University (GU-481).

References

1 Cooke RM, Wilson AM, Tuomisto JT, Morales O, Tainio M, Evans J: A probabilistic characterization of the relationship between fine particulate matter and mortality: elicitation of European experts: Environ Sci Technol 2007;41(18):6598–6605.

2 Nag S, Gupta AK, Mukhopadhyay UK: Size distribution of atmospheric aerosols in Kolkata, India and the assessment of pulmonary deposition of particle mass: Indoor Built Environ 2005;14(5):381–389.

3 WHO: Air Quality Guidelines for Particulate Matter, Ozone, Nitrogen, Dioxide and Sulfur Dioxide, Global Update 2005, Summary of Risk Assessment. Geneva, Switzerland, World Health Organization, 2006.

4 Charron A, Harrison RM: Fine ($PM_{2.5}$) and coarse ($PM_{2.5–10}$) particulate matter on a heavily trafficked London Highway: sources and processed: Environ Sci Technol 2005;39:7768–7776.

5 Cheng Y, Lee SC, Ho KF, Chow JC, Watson JG, Louie PKK, Cao JJ, Hai X: Chemically-speciated on-road $PM_{2.5}$ motor vehicle emission factor in Hong Kong: Sci Total Environ 2010;408(7):1621–1627.

6 Saksena S, Uma R: Longitudinal study of indoor particulate matter and its relationship to outdoor concentration in New Delhi, India: Indoor Built Environ 2008;17(6):543–551.

7 Diapouli E, Chaloulakou A, Spyrellis N: Indoor and outdoor particulate matter concentrations at school in the Athens areas: Indoor Built Environ 2007;16(1):55–61.

8 Loupa G, Kioutsioukis I, Rapsomanikis S: Indoor-outdoor atmospheric particulate matter relationships in naturally ventilated offices: Indoor Built Environ 2007;16(1):63–69.

9 Abdul-Wahab SA: Indoor and outdoor relationships of atmospheric particulates in Oman: Indoor Built Environ 2006;15(3):247–255.

10 Branis M, Hovorka J, Rezacova P, Domasova M, Lazaridis M: Effect of indoor and outdoor sources on particulate matter concentrations in a naturally ventilated flat (URBAN-AEROSOL Project, Prague): Indoor Built Environ 2005;14(3–4):307–312.

11 El-Hougeiri N, El-Fadel M: Correlation of indoor-outdoor air quality in urban areas: Indoor Built Environ 2004;13(6):421–431.

12 Mohammadyan M, Ashmore MR: Personal exposure and indoor $PM_{2.5}$ concentrations in an urban population: Indoor Built Environ 2005;14(3–4):313–320.

13 Aleksandropoulou V, Mitsakou C, Housiadas C, Lazaridis M: Particulate matter exposure and dose relationships derived from realistic exposure scenarios: Indoor Built Environ 2008;17(3):237–246.

14 Zhang Y, Zhao B, Li X: Perceived particle intensity: an indicator to evaluate indoor particle pollution: Indoor Built Environ 2006;15(2):155–164.

15 Khallare PS, Pandey R, Balachandran S: Characterisation of indoor PM_{10} in residential areas of Delhi: Indoor Built Environ 2004;13(2):139–147.

16 Ahmad K, Khare M, Chaudhry KK: Wind tunnel simulation studies on dispersion at urban street canyons and intersections: a review: J Wind Eng Ind Aerodyn 2005;9:697–711.

17 Pavageau M, Schatzmann M: Wind tunnel measurements of concentration fluctuations in an urban street canyon: Atmos Environ 1999;24–25:3961–3971.

18 Vardoulakis S, Fisher BEA, Pericleous K, Gonzalez-Flesca N: Modelling air quality in street canyons: a review: Atmos Environ 2003;37(2):155–182.

19 Park SK, Kim SD, Lee H: Dispersion characteristics of vehicle emission in street canyons: Sci Total Environ 2004;324(1–3):263–271.

20 Chan AT, So ESP, Samad SC: Strategies guidelines for street canyon geometr to achieve sustainable street air quality: Atmos Environ 2001;35(32):5681–5691.

21 Xie XM, Wang JS, Huang Z: Traffic emission transportation in street canyons: J Hydrodyn Ser B 2009;21(1):108–117.

22 Morena F, Favale G, Vardoulakis S, Solezzo E: Modelling dispersion of traffic pollution in a deep street canyon: application of CFD and operational models: Atmos Environ 2009;43(14):2303–2311.

23 Chan LY, Kwok WS: Vertical dispersion of suspended particulates in urban area of Hong Kong: Atmos Environ 2000;34:4403–4412.

24 Li XL, Wang JS, Tu, XD, Liu W, Huang Z: Vertical variations of particle number concentration and size distribution in a street canyon in Shanghai, China: Sci Total Environ 2007;378(3):306–316.

25 Cai XM, Barlow JF, Belcher SE: Dispersion and transfer of passive scalars in and above street canyons—large-eddy simulations: Atmos Environ 2008;42:5885–5895.

26 Cui ZQ, Cai XM, Baker CJ: Large-eddy simulation of turbulent flow in a street canyon: Q J R Meteorolog Soc 2004;130(599):1373–1394.

27 Li XX, Liu CH, Leung DYC: Numerical investigation of pollutant transport characteristics inside deep urban street canyons: Atmos Environ 2009;43:2410–2418.

28 Yang Y, Shao Y: Numerical simulations of flow and pollutant dispersion in urban atmospheric boundary layers: Environ Modeling Assess 2008;23:906–921.

29 Eliasson I, Offerle B, Grimmond CSB, Lindqvist S: Wind fields and turbulence statistics in an urban street canyon: Atmos Environ 2006;40(1):1–16.

30 Li XX, Liu CH, Leung DYC, Lam KM: Physical modeling of flow field inside urban street canyons: J Appl Meteorol Climatol 2008;41:2058–2067.

31 Hoydysh WG, Griffiths RA, Ogawa Y: A scale model study of the dispersion of pollutant in street canyons: in the 67th Annual Meeting of the Air Pollution Control Association, Denver, CO, 1974.

32 Uehara K, Wakamatu S, Ooka R: Studies on critical Reynolds number indices for wind-tunnel experiments on flow within urban area: Boundary Layer Meteorol 2003;107:353–370.

33 Schatzmann M, Frantz H, Grawe D, Leitl B, Mueller WJ: Do field data represent the truth?: in Proceedings of the Third Intrnational Conference on Urban Air Quality, Loutraki, Greece, 2001.

34 Solazzo E, Cai XM, Vardoulakis S: Modelling wind flow and vehicle-induced turbulence in urban streets: Atmos Environ 2008;42:4918–4931.

35 Sagaut P: Large Eddy Simulation for Incomprassible Flows. Heidelberg, Springer, 2002.

36 Qiu J, Gu ZL, Wang ZS: Numerical study of the response of an atmospheric surface layer to a spatially nonuniform plant canopy: Boundary Layer Meteorol 2008;127:293–311.

37 Zhao B, Li X, Zhang Z: Numerical study of particle deposition in two ventilated rooms: Indoor Built Environ 2004;13:443–451.

38 Zhao B, Wu P. Song F, Yan D, Yang X, Li X, Jiang Y: Numerical simulation of indoor PM distribution over the whole year by zonal model: Indoor Built Environ 2004;13:453–462.

39 Klein PK, Plate EJ: Wind-tunnel study of concentration fields in street canyons: Atmos Environ 1999;33:3373–3979.

40 Pavageau M, Schatzmann M: Wind tunnel measurements of concentration fluctuations in an urban street canyon: Atmos Environ 1999;33(24–25):3961–3971.

41 Colls JJ, Micallef A: Measured and modelled concentrations and vertical profiles of airborne particulate matter within the boundary layer of a street canyon: Sci Total Environ 1999;235(1–3):221–233.

42 Kumar P, Garmory A, Ketzel M, Berkowicz R, Britter R: Comparative study of measured and modelled number concentrations of nanoparticles in an urban street canyon: Atmos Environ 2009;43(4):949–958.

43 Wu Y, Hao JM, Fu LX, Wang ZS, Tang U: Vertical and horizontal profiles of air borne particulate matter near roads in Macao, China: Atmos Environ 2002;36(31):4907–4918.

44 Tao WQ: Recent Advancement in Numerical Heat Transfer. Beijing, China, Science Press, 2005.

45 Smagorinsky J: General circulation experiments with the primitive equations: Part 1. The basic experiment: Mon Weather Rev 1963;91:99–164.

46 Hinds WC: Aerosol Technology. New York, John Wiley & Sons, 1982.

47 Cheng Y, Lee SC, Ho KF, Louie PKK: On-road particulate matter ($PM_{2.5}$) and gaseous emissions in the Shing Mun Tunnel, Hong Kong: Atmos Environ 2006;40:4235–4245.

48 Katolicky J, Jicha M: Eulerian–Largangian model for traffic dynamics and its impact on operational ventilation of road tunnels: J Wind Eng Ind Aerodyn 2005;93:61–77.

49 Walton A, Cheng AYS: Large-eddy simulation of pollution dispersion in an urban street canyon—Part II: idealised canyon simulation: Atmos Environ 2002;36(22):3615–3627.

50 Li XX, Liu CH, Leung DYC: Large-eddy simulation fo flow and pollutant dispersion in high-aspect-ratio urban street canyons with wall model: Boundary Layer Meteorol 2008;129:249–268.